

1 **Cultivation and characterization of a novel clade of deep-sea Chloroflexi:**
2 **providing a glimpse of the phylum Chloroflexi involved in sulfur cycling**

3 Rikuan Zheng^{1,2,3,4}, Ruining Cai^{1,2,3,4}, Rui Liu^{1,2,4}, Yeqi Shan^{1,2,3,4}, Ge Liu^{1,2,4}, Chaomin Sun^{1,2,4*}

4 ¹CAS Key Laboratory of Experimental Marine Biology & Center of Deep Sea
5 Research, Institute of Oceanology, Chinese Academy of Sciences, Qingdao, China

6 ²Laboratory for Marine Biology and Biotechnology, Qingdao National Laboratory
7 for Marine Science and Technology, Qingdao, China

8 ³College of Earth Science, University of Chinese Academy of Sciences, Beijing,
9 China

10 ⁴Center of Ocean Mega-Science, Chinese Academy of Sciences, Qingdao, China

11

12 * Corresponding author

13 Chaomin Sun Tel.: +86 532 82898857; fax: +86 532 82898857.

14 E-mail address: sunchaomin@qdio.ac.cn

15

16

17 **Key words:** Chloroflexi, deep sea, cultivation, sulfur cycle, novel class

18 **Running title:** Chloroflexi bacteria contribute to sulfur cycle

19

20

21 **Abstract**

22 Chloroflexi bacteria are abundant and globally distributed in various unexplored
23 biospheres on Earth. However, only few Chloroflexi members have been cultivated,
24 hampering further understanding of this important group. In the current study, we
25 firstly clarify the high abundance of the phylum Chloroflexi in deep-sea sediments via
26 the operational taxonomic units analysis. We further successfully isolate a novel
27 Chloroflexi strain ZRK33 from cold seep sediments by using an enrichment medium
28 constantly supplemented with rifampicin. Phylogenetic analyses based on 16S rRNA
29 gene, genome, RpoB and EF-tu proteins indicate that strain ZRK33 represents a novel
30 class, and the class is designated as Sulfochloroflexia because whole set of genes
31 encoding key enzymes responsible for assimilatory sulfate reduction are identified in
32 the genome of strain ZRK33. Indeed, assimilation of sulfate or thiosulfate by strain
33 ZRK33 evidently benefits its growth and morphogenesis. Proteomic results suggest
34 that metabolization of sulfate or thiosulfate significantly promotes the transport and
35 degradation of various macromolecules and thereby stimulating the energy production.
36 Notably, the putative genes associated with assimilatory and dissimilatory sulfate
37 reduction ubiquitously distribute in the metagenome-assembled genomes of 27
38 Chloroflexi members derived from deep-sea sediments, strongly suggesting that
39 Chloroflexi bacteria play undocumented key roles in deep-sea sulfur cycling.

40

41

42 **Introduction**

43 Deep marine subsurface is one of the least-understood habitats on Earth and is
44 estimated to contain up to 3×10^{29} microbial cells, which is equivalent to the combined
45 microbial biomass of the oceanic water column and terrestrial soil [1]. The
46 prokaryotic biomass in deep marine subsurface sediments exceeds 10^5 microbial
47 cells/cm³ even at depths of nearly to 1,000 m below the seafloor [2,3]. These
48 microorganisms are the primary drivers of elemental cycles within deep marine
49 subsurface sediments and play key roles in the recycling of biogeochemical nutrients
50 to the water column [4]. Members of the phylum Chloroflexi widely distributed in
51 various environments with high abundance, for example, in some marine subsurface
52 sediments the number of Chloroflexi bacteria is shown to be closely equivalent to
53 other total bacterial counts [3,5-8], strongly suggesting that the phylum Chloroflexi is
54 an essential group to maintain the population equilibrium of marine subsurface
55 ecosystems [9-12].

56 The phylum Chloroflexi, formerly called the ‘green nonsulfur bacteria’, is a
57 remarkably diverse, deeply branching lineage in the domain Bacteria [13]. Currently,
58 the phylum Chloroflexi is divided phylogenetically into nine classes, including
59 Chloroflexia [14], Anaerolineae [15], Caldilineae [15], Ktedonobacteria [16],
60 Thermomicrobia [17], Dehalococcoidia [18], Tepidiformia [19], Thermoflexia [20]
61 and Ardenticatenia [21]. Concomitant with the expansion of the phylum Chloroflexi
62 by cultivation, studies utilizing cultivation-independent techniques have revealed a

63 remarkable diversity of as-yet uncultivated microorganisms affiliated with the phylum
64 Chloroflexi [22], indicating immeasurable novel lineages of Chloroflexi existing in
65 nature. Despite the Chloroflexi bacteria being among the first widespread microbial
66 lineages discovered in deep-sea environments we still lack cultured representatives
67 (especially those with relative fast growing rate) for this group and their detailed
68 physiological, genetic and ecological properties are currently almost completely
69 obscure [13,23,24]. For example, until now, only basic physiological characteristics
70 of two cultured strains of Chloroflexi with extremely slow growth rate (doubling time
71 from 1.5 days to 19 days) from the deep-sea sediments are available [10,23], and their
72 central metabolisms and contributions to biogeochemical processes including sulfur
73 cycling are largely unknown.

74 The cycling of sulfur is one of Earth's major biogeochemical processes and is
75 closely related to the energy metabolism of microorganisms living in the cold seep
76 and hydrothermal vents [25-27]. Importantly, the coupling of sulfate/sulfite reduction
77 to oxidation of H₂, small chain fatty acids, or other carbon compounds limits the
78 availability of these substrates to other organisms like methanogens and alters the
79 energetics via syntrophic interactions, and thereby impacting the methane production
80 [25]. Given the importance of sulfur cycling in the deep biospheres, it is vital that we
81 understand which organisms can carry out the reactions and the pathways involved
82 [27]. Based on metagenomic sequencing results, some SAR202 members of the
83 phylum of Chloroflexi are predicted to be sulfite-oxidizers, making them as potential

84 key players in the sulfur cycle at the deep marine environment [28]; based on
85 single-cell genomic sequencing results, some members of Dehalococcoidia class
86 within the phylum Chloroflexi are demonstrated to possess diverse genes encoding
87 dissimilatory sulfite reductase [4], suggesting that Dehalococcoidia bacteria could
88 drive sulfite reduction and respire oxidized sulfur compounds. Together, some of the
89 members of Chloroflexi are believed to play a previously unrecognized role in sulfur
90 cycling, which needs to be verified with cultured representatives of Chloroflexi
91 isolated from deep-sea environments.

92 In this study, we checked the abundance of Chloroflexi existing in both deep-sea
93 cold seep and hydrothermal vents. Using an enrichment medium continuously
94 supplemented with rifampicin pressure, we have successfully isolated a novel member
95 of Chloroflexi, strain ZRK33, from the deep marine subsurface sediments collected
96 from a typical cold seep in the South China Sea (1,146 m water depth). Strain ZRK33
97 is further to shown to be a representative of a novel class of the phylum Chloroflexi,
98 designated as Sulfochloroflexia given that strain ZRK33 is demonstrated to assimilate
99 sulfate and thiosulfate. Lastly, the broad distribution of diverse genes encoding key
100 enzymes driving both sulfur assimilatory and dissimilatory reduction in the
101 metagenome-assembled genomes from deep-sea sediments is detailed analyzed.

102 **Materials and methods**

103 **Sampling and operational taxonomic units (OTUs) analysis**

104 The deep-sea sediment samples were collected by *RV KEXUE* from a typical cold
105 seep in the South China Sea (E 119°17'07.322", N 22°06'58.598") at a depth of
106 approximately 1,146 m and two hydrothermal vent fields in the Okinawa Trough (E
107 126°53'50.247", N 27°47'11.096"; E 124°22'24.86", N 25°15'47.438") in July of 2018
108 as described previously [26]. In order to understand the abundance of Chloroflexi
109 phylum in the deep-sea sediments, we selected eight sedimentary samples (six cold
110 seep samples including RPC, ZC1, ZC2, ZC3, ZC4 and ZC5 at depth intervals of 0-10,
111 30-50, 90-110, 150-170, 210-230 and 230-250 cm, respectively; two hydrothermal
112 vents samples including H1 and H2 at depth intervals of 0-20 cm) for OTUs
113 sequencing performed by Novogene (Tianjin, China). Briefly, total DNAs from these
114 samples were extracted by the CTAB/SDS method [29] and diluted to 1 ng/μL with
115 sterile water and used for PCR template. 16S rRNA genes of distinct regions (16S
116 V3/V4) were amplified using specific primers (341F: 5'-
117 CCTAYGGGRBGCASCAG and 806R: 5'- GGACTACNNGGGTATCTAAT). The
118 PCR products were purified with a Qiagen Gel Extraction Kit (Qiagen, Germany) for
119 libraries construction. Sequencing libraries were generated using TruSeq® DNA
120 PCR-Free Sample Preparation Kit (Illumina, USA) following the manufacturer's
121 instructions. The library quality was assessed on the Qubit® 2.0 Fluorometer
122 (Thermo Scientific, USA) and Agilent Bioanalyzer 2100 system. The library was
123 sequenced on an Illumina NovaSeq platform and 250 bp paired-end reads were
124 generated. Paired-end reads were merged using FLASH (V1.2.7,

125 <http://ccb.jhu.edu/software/FLASH/>) [30], which was designed to merge paired-end
126 reads when at least some of the reads overlap with those generated from the opposite
127 end of the same DNA fragments, and the splicing sequences were called raw tags.
128 Quality filtering on the raw tags was performed under specific filtering conditions to
129 obtain the high-quality clean tags [31] according to the QIIME (V1.9.1,
130 http://qiime.org/scripts/split_libraries_fastq.html) quality controlled process. The tags
131 were compared with the reference database (Silva database, <https://www.arb-silva.de/>)
132 using UCHIME algorithm (UCHIME Algorithm,
133 http://www.drive5.com/usearch/manual/uchime_algo.html) [32] to detect chimera
134 sequences, and then the chimera sequences were removed [33]. Sequence analyses
135 were performed by Uparse software (Uparse v7.0.1001, <http://drive5.com/uparse/>)
136 [34]. Sequences with $\geq 97\%$ similarity were assigned to the same OTUs. The
137 representative sequence for each OTU was screened for further annotation. For each
138 representative sequence, the Silva Database (<http://www.arb-silva.de/>) [35] was used
139 based on Mothur algorithm to annotate taxonomic information.

140 **Metagenomic sequencing, assembly, binning and annotation**

141 To understand the common characteristics of Chloroflexi in deep-sea environments,
142 four cold seep sediment samples (zhu, C1, C2 and C4) and two hydrothermal vents
143 sediment samples (H1 and H2) were selected for metagenomic analysis in BGI (BGI,
144 China). Briefly, total DNAs from these samples (20 g each) were extracted using the
145 Qiagen DNeasy® PowerSoil® Pro Kit (Qiagen, Hilden, Germany) and the integrity of

146 DNA was evaluated by gel electrophoresis. Then 0.5 μ g DNA of each sample was
147 used library construction. The library was prepared with an amplification step for
148 each sample. And then DNAs were cleaved into 50~800 bp fragments by the Covaris
149 E220 ultrasonicator (Covaris, Brighton, UK) and some fragments between 150~250
150 bp were selected using AMPure XP beads (Agencourt, USA) and repaired using T4
151 DNA polymerase (Enzymatics, USA). All next-generation sequencing (NGS) was
152 performed on the BGISEQ-500 platform (BGI, Qingdao, China) and generated 100 bp
153 paired-end raw reads. Quality control was performed by SOAPnuke (v1.5.6) (setting:
154 -l 20 -q 0.2 -n 0.05 -Q 2 -d -c 0 -5 0 -7 1) [36] and the clean data were assembled
155 using MEGAHIT (v1.1.3) (setting:--min-count 2 --k-min 33 --k-max 83 --k-step 10)
156 [37]. Assemblies of these samples were automatically binned using Maxbin2 [38],
157 metaBAT2 [39] and Concoct [40]. MetaWRAP [41] was used to purify and organize
158 data to generate the final bins. Finally, the completeness and contamination of
159 metagenome-assembled genomes (MAGs) were assessed by the checkM (v1.0.18)
160 [42]. These obtained MAGs were subsequently annotated by searching these
161 predicted genes against KEGG (Release 87.0), NR (20180814), Swissprot
162 (release-2017_07) and COG (update-2018_08) databases. Additionally, we utilized a
163 custom hmmer as well as the Pfam and TIGRFAM databases to search for genes
164 associated with sulfur metabolism using hmmsearch (e-value cut-off of 1e-20) [43].

165 **Enrichment and cultivation of deep-sea Chloroflexi bacteria**

166 To enrich the Chloroflexi bacteria, deep-sea sediment samples were cultured at 28 °C
167 for one month in an anaerobic enrichment medium (containing 1.0 g/L NH₄Cl, 1.0 g/L
168 NaHCO₃, 1.0 g/L CH₃COONa, 0.5 g/L KH₂PO₄, 0.2 g/L MgSO₄·7H₂O, 1.0 g/L yeast
169 extract, 1.0 g/L peptone, 0.7 g/L cysteine hydrochloride, 500 µL/L 0.1 % (w/v)
170 resazurin, pH 7.0) with 50 µg/mL rifampicin. This medium was prepared
171 anaerobically as previously described and named ORG in this study [44]. A 50 µL
172 enrichment culture was spread on the Hungate tubes containing ORG broth
173 supplemented with 15 g/L agar after 10,000 times dilution. These Hungate tubes were
174 anaerobically incubated at 28 °C for 7 days. Individual colonies were respectively
175 picked using sterilized bamboo sticks and then cultured in the ORG broth. Strain
176 ZRK33 was isolated and purified by repeated use the Hungate roll-tube methods for
177 several rounds until it was considered to be axenic. The purity of strain ZRK33 was
178 confirmed by transmission electron microscopy (TEM) and repeated partial
179 sequencing of the 16S rRNA gene. Strain ZRK33 was preserved at -80 °C in ORG
180 broth supplemented with 20% (v/v) glycerol.

181 **TEM observation**

182 To observe the morphological characteristics of strain ZRK33, the cell suspension of
183 fresh culture was collected at 5,000 ×g for 10 min and washed with Milli-Q water,
184 and then taken by immersing copper grids coated with a carbon film for 10 min.
185 Thereafter, the copper grids were washed for 10 min in Milli-Q water and dried for 20
186 min at room temperature [45]. Ultrathin-section electron microscopic observation was

187 performed as described previously [46-48]. The sample was firstly preserved in 2.5%
188 (v/v) glutaraldehyde for 8 h at 4 °C, washed three times with phosphate buffer saline
189 (PBS) and then dehydrated in ethanol solutions of 30%, 50%, 70%, 90% and 100%
190 for 10 min each time. Finally, the sample was embedded in a plastic resin. Ultrathin
191 sections (50~70 nm) of cells were prepared with an ultramicrotome (Leica EM UC7,
192 Gemany), stained with uranyl acetate and lead citrate. All of these samples were
193 examined using TEM (HT7700, Hitachi, Japan) with a JEOL JEM 12000 EX
194 (equipped with a field emission gun) at 100 kV.

195 **Genome sequencing and genomic analysis**

196 Genomic DNAs of strain ZRK33 were extracted from 2 L cells that cultured for 7
197 days at 28 °C. The DNA library was prepared using the Ligation Sequencing Kit
198 (SQK-LSK109, UK), and sequenced using a FLO-MIN106 vR9.4 flow-cell for 48 h
199 on MinKNOWN software v1.4.2 (Oxford Nanopore Technologies, UK).
200 Whole-genome sequence determinations of strain ZRK33 were carried out with the
201 Oxford Nanopore MinION (Oxford, UK) and Illumina MiSeq sequencing platform
202 (San Diego, CA). A hybrid approach was utilized for genome assembly using reads
203 from both platforms. Base-calling was performed using Albacore software v2.1.10
204 (Oxford Nanopore Technologies, UK). Nanopore reads were processed using
205 protocols toolkit for quality control and downstream analysis [49]. Filtered reads were
206 assembled using Canu version 1.8 [50] with the default parameters for Nanopore data.

207 Finally, the genome was assembled into a single contig and was manually circularized
208 by deleting an overlapping end.

209 The genome relatedness values were calculated by multiple approaches: Average
210 Nucleotide Identity (ANI) based on the MUMMER ultra-rapid aligning tool (ANIm),
211 ANI based on the BLASTN algorithm (ANIb), the tetranucleotide signatures (Tetra),
212 and *in silico* DNA-DNA similarity. ANIm, ANIb and Tetra frequencies were
213 calculated using JSpecies WS (<http://jspecies.ribohost.com/jspeciesws/>) [51]. The
214 recommended species criterion cut-offs were used: 95% for the ANIb and ANIm and
215 0.99 for the Tetra signature. The *in silico* DNA-DNA similarity values were
216 calculated by the Genome-to-Genome Distance Calculator (GGDC)
217 (<http://ggdc.dsmz.de/>) [52]. The *isDDH* results were based on the recommended
218 formula 2, which is independent of genome size.

219 **Phylogenetic analysis**

220 The full-length 16S rRNA gene sequence (1,489 bp) of strain ZRK33 was extracted
221 from the genome, which had been deposited in the GenBank database (accession
222 number MN817941), and other related taxa used for phylogenetic analysis were
223 obtained from NCBI (www.ncbi.nlm.nih.gov/). The genome tree was constructed
224 from a concatenated alignment of 37 protein-coding genes [53] that extracted from
225 each genome by Phylosift (v1.0.1) [54], all of which were in a single copy and
226 universally distributed in both archaea and bacteria (Supplementary Table S1). The
227 genomes used to construct the genome tree included both draft and finished genomes

228 from the NCBI databases. The RpoB and EF-tu tree was constructed by using RpoB
229 or EF-tu protein sequences, which were identified from 49 genomes using the hidden
230 markov models (HMMs) TIGR02029 and TIGR00485 from TIGRfams
231 (<http://www.jcvi.org/cgi-bin/tigrfams/index.cgi>), respectively. Phylogenetic trees
232 were constructed by using W-IQ-TREE web server (<http://iqtree.cibiv.univie.ac.at>)
233 [55] with LG+F+I+G4 model. The online tool Interactive Tree of Life (iTOL v5)
234 [56,57] was used for editing trees.

235 **Growth assays of strain ZRK33**

236 Growth assays were performed at atmospheric pressure. Briefly, 15 mL fresh strain
237 ZRK33 culture was inoculated in 2 L Hungate bottles containing 1.5 L ORG broth
238 supplemented with 20 mM Na₂SO₄, 200 mM Na₂SO₄, 20 mM Na₂S₂O₃, 200 mM
239 Na₂S₂O₃, 1 mM Na₂SO₃ and 1 mM Na₂S, respectively. Each condition had three
240 replicates. These Hungate bottles were then anaerobically incubated at 28 °C for 12 d.
241 Bacterial growth status was monitored by measuring the OD₆₀₀ value every 12 h until
242 cell growth reached the stationary phase. For the morphological observation of strain
243 ZRK33, we took 20 µL culture that cultivated for 12 d, which was then checked and
244 recorded under an inverted microscope (NIKON TS100, Tokyo, Japan) equipped with
245 a digital camera. For the determination of the dynamics of the concentrations of
246 Na₂SO₄ and Na₂S₂O₃ in the culture, we selected three cultivation time points at 5 d, 8
247 d and 12 d, respectively, and each condition had three replicates. The supernatant was
248 collected at 12,000 g for 10 min and diluted 80 times, and the concentrations of SO₄²⁻

249 and $S_2O_3^{2-}$ in the diluted supernatant were respectively measured by the ion
250 chromatograph (ECO IC, Herisau, Switzerland) with an chromatographic column
251 (Metrosep A Supp5). The column was eluted with mobile phase A (3.2 mmol/L
252 Na_2CO_3) and mobile phase B (1.0 mmol/L $NaHCO_3$) at 25 °C.

253 **Proteomic analysis**

254 Proteomic analysis was performed by PTMBiolabs (Hangzhou, China). Briefly, strain
255 ZRK33 was respectively cultivated in the ORG broth (set as the control group and
256 indicated as “C”), ORG broth supplemented with 200 mM Na_2SO_4 (set as the
257 experimental group and indicated as “S”) and 200 mM $Na_2S_2O_3$ (set as the
258 experimental group and indicated as “T”) for 8 d at 28 °C. Then the cells were
259 collected and sonicated three times on ice using a high intensity ultrasonic processor
260 in lysis buffer (8 M urea, 1% Protease Inhibitor Cocktail). The remaining debris was
261 removed by centrifugation at 12,000 g at 4 °C for 10 min. Finally, the supernatant was
262 collected and the protein concentration was determined with a BCA kit (Solarbio,
263 China) according to the instructions. The detailed protocols of proteomics sequencing
264 technology were described in the Supplementary information. The heat map was
265 made by HemI 1.0 based on the KEGG enrichment results.

266 **Data availability**

267 The raw amplicon sequencing data have been deposited to NCBI Short Read Archive
268 (accession numbers: PRJNA675395 and PRJNA688815). The BioProject accession
269 number of metagenome-assembled genomes (MAGs) of Chloroflexi bacteria used in

270 this study is PRJNA667788. The full-length 16S rRNA gene sequence of *S.*
271 *methaneseepsis* ZRK33 has been deposited at GenBank under the accession number
272 MN817941. The complete genome sequence of *S. methaneseepsis* ZRK33 has been
273 deposited at GenBank under the accession number CP051151. The mass spectrometry
274 proteomics data have been deposited to the Proteome Xchange Consortium with the
275 dataset identifier PXD023380.

276 **Results**

277 **Chloroflexi bacteria possess high abundance in the deep-sea environments**

278 To gain preliminary insights of Chloroflexi bacteria existing in the deep-sea
279 environments, OTUs sequencing was firstly performed to detect the abundance of the
280 phylum Chloroflexi present in the cold seep sediments at depth intervals of 0-10 cm
281 (sample RPC), 30-50 cm (sample ZC1), 90-110 cm (sample ZC2), 150-170 cm
282 (sample ZC3), 210-230 cm (sample ZC4), 230-250 cm (sample ZC5) and
283 hydrothermal vents sediments at depth intervals of 0-20 cm from the surface to the
284 deep layer in two different sampling sites (samples H1 and H2). As previously
285 reported [2,6,7], the Chloroflexi group was both the second most abundant phylum in
286 cold seep and hydrothermal vents sediments, suggesting Chloroflexi was dominant in
287 these deep-sea regions (Figs. 1A and 1B). The proportion of Chloroflexi respectively
288 accounted for 6.15%, 10.92%, 5.04%, 8.67% and 13.67% of the whole bacterial
289 domain at the phylum level in samples RPC, ZC1, ZC2, H1 and H2 (Figs. 1A and 1B).

290 Moreover, the ratio of the phylum Chloroflexi to the whole bacteria domain is much
291 higher in the top layer than that in the bottom one, providing a preliminary hint of
292 distribution of Chloroflexi bacteria in the deep-sea sediments. To obtain further
293 insights into the deep-sea Chloroflexi bacteria, we analyzed the abundance of
294 Chloroflexi members at the class level and found that Dehalococcoidia and
295 Anaerolineae were the top two classes in the cold seep (Fig. 1C) and hydrothermal
296 vents sediments (Fig. 1D). In particular, Dehalococcoidia class bacteria are an
297 absolute dominant population in 7 of 8 samples, strongly suggesting the importance of
298 this lineage in deep-sea environments.

299 **Cultivation and morphology of a novel Chloroflexi bacterium isolated from the** 300 **deep-sea cold seep**

301 To culture novel isolates belonging to the phylum Chloroflexi from deep-sea
302 environments, we improved the enrichment method by using a specific medium that
303 constantly supplemented with 50 µg/mL rifampicin, given that many members of
304 Chloroflexi were reported to tolerate rifampicin [13,23] while most of other bacteria
305 are sensitive to this antibiotics. Using this strategy, we anaerobically enriched the
306 deep-sea sediment samples at 28 °C for one month. Thereafter, the enriched samples
307 were plated on solid medium in Hungate tubes, and individual colonies with distinct
308 morphology were picked and cultured (Fig. 2A). Excitingly, some of the cultured
309 colonies were identified as Chloroflexi bacteria based on their 16S rRNA sequences.
310 Among them, strain ZRK33 possessed a fast growth rate and was chosen for further

311 study. Under TEM observation, the cells of strain ZRK33 were filamentous, generally
312 more than 20 μm long and 0.5-0.6 μm wide, and had no flagellum (Figs. 2B and 2C).
313 Ultrathin sections of whole cells of strain ZRK33 revealed a cytoplasmic membrane
314 surrounded by a cell wall surface layer (Figs. 2D and 2E). The strain did not possess a
315 clearly visible sheath-like structure (Fig. 2D) as shown in the *Pelolinea submarina*
316 strain MO-CFX1^T, a typical Chloroflexi bacterium belonging to the class
317 Anaerolineae [23]. Based on the 16S rRNA sequence of strain ZRK33, a sequence
318 similarity calculation using the NCBI server indicated that the closest relatives of
319 strain ZRK33 were *Anaerolinea thermophila* UNI-1 (82.75%) (class Anaerolineae),
320 *Ornatilinea apprima* P3M-1 (82.32%) (class Anaerolineae), *Thermomarinilinea*
321 *lacunifontana* SW7 (82.42%) (class Anaerolineae) and *Caldilinea aerophila* DSM
322 14535 (81.87%) (class Cadilineae). Recently, taxonomic thresholds based on 16S
323 rRNA gene sequence identity values were suggested [58]: for classes, the proposed
324 thresholds for median and minimum sequence identity values were 86.35% and
325 80.38%, respectively. Based on these criteria, we propose that strain ZRK33 might be
326 a representative of a novel class-level Chloroflexi.

327 **Genomic characteristics and phylogenetic analysis of strain ZRK33**

328 To understand more characteristics of strain ZRK33, its whole genome was sequenced
329 and analyzed. The genome size of strain ZRK33 was 5,631,885 bp with a DNA G+C
330 content of 52.76% (Fig. 3A and Supplementary Table S2). Annotation of the genome
331 of strain ZRK33 revealed it consisted of 4,885 predicted genes that included 55 RNA

332 genes (6 rRNA genes, 46 tRNA genes and 3 other ncRNAs). When exploring the
333 detailed genomic composition of strain ZRK33, we found that various genes encoding
334 key enzymes responsible for sulfur metabolism existing in the genome of ZRK33 (Fig.
335 3B). And these enzymes are thought to involve in assimilatory sulfate reduction,
336 strongly indicating that strain ZRK33 might be a representative of a novel clade that
337 driving deep-sea sulfur cycling.

338 To further clarify the phylogenetic position of strain ZRK33, the genome
339 relatedness values were calculated by the average nucleotide identity (ANI), *in silico*
340 DNA-DNA similarity (*is*DDH) and the tetranucleotide signatures (Tetra), against six
341 genomes (strain ZRK33, and five strains MO-CFX2, MO-CFX1, UNI-1, IMO-1 and
342 P3M-1 belonging to class Anaerolineae) (Supplementary Table S3). The average
343 nucleotide identities (ANIB) of ZRK33 with strains MO-CFX2, MO-CFX1, UNI-1,
344 IMO-1 and P3M-1 were 64.81%, 63.06%, 63.42%, 63.41% and 63.29%, respectively.
345 The average nucleotide identities (ANIm) of ZRK33 with MO-CFX2, MO-CFX1,
346 UNI-1, IMO-1 and P3M-1 were 85.21%, 82.63%, 83.42%, 83.15% and 83.23%,
347 respectively. The tetra values of ZRK33 with MO-CFX2, MO-CFX1, UNI-1,
348 IMO-1 and P3M-1 were 0.48145, 0.67572, 0.64677, 0.65234 and 0.65126. Based on
349 digital DNA-DNA hybridization employing the Genome-to-Genome Distance
350 Calculator GGDC, the *in silico* DDH estimates for ZRK33 with MO-CFX2,
351 MO-CFX1, UNI-1, IMO-1 and P3M-1 were 23.30%, 24.20%, 20.40%, 21.60% and
352 23.80%, respectively. These results together demonstrated the genome of strain

353 ZRK33 to be obviously below established ‘cut-off’ values (ANIb: 95%, ANIm: 95%,
354 isDDH: 70%, Tetra: 0.99) for defining bacterial species, suggesting strain ZRK33
355 represents a novel taxon within the phylum Chloroflexi as currently defined.

356 To further confirm the taxonomic status of strain ZRK33, we performed the
357 phylogenetic analyses with 16S rRNA genes from all cultured Chloroflexi
358 representatives, some uncultured SAR202 representatives and other uncultured
359 Chloroflexi bacteria. The maximum likelihood tree of 16S rRNA placed strain ZRK33
360 as a sister of the strain MO-CFX2, which together formed a distinct cluster separating
361 from other classes of the phylum Chloroflexi (Fig. 4). Furthermore, the genome tree
362 also placed the novel clade as a sister of the Anaerolineae class belonging to the
363 phylum Chloroflexi (Supplementary Figure S1). The phylogenetic analysis of strain
364 ZRK33 using the beta subunit of RNA polymerase (RpoB), which also showed that
365 the novel clade formed a separate branch from the Anaerolineae class (Supplementary
366 Figure S2). More importantly, the broader phylogeny of elongation factor Tu (EF-Tu)
367 supported the placement of the novel clade within the phylum Chloroflexi
368 (Supplementary Figure S3). Based on phylogenetic, genomic and phenotypic
369 characteristics, we proposed that strain ZRK33 together with strain MO-CFX2
370 (previously classified as a representative of a novel order of class Anaerolineae) were
371 classified as the type strains of a new class of the phylum Chloroflexi. Given the
372 broad distribution of genes associated with sulfur metabolism in the genome of strain
373 ZRK33 (Fig. 3B) and its significant potential involved in sulfur cycling, we propose

374 Sulfochloroflexia classis nov., Sulfochloroflexales ord. nov., Sulfochloroflexaceae
375 fam. nov. and *Sulfochloroflexus methaneseepsis* gen. nov.

376 **Description of *Sulfochloroflexus* gen. nov. and *Sulfochloroflexus methaneseepsis***
377 **sp. nov.**

378 *Sulfochloroflexus* (Sul.fo'ch.lo.ro.fle.xus. N.L. fem. pl. n. Sulfo, sulfur; N.L. masc.
379 *chloroflexus* a bacterial genus; N.L. masc. n. *Sulfochloroflexus*, *chloroflexus* sulfur
380 loving. Facultatively anaerobic, mesophilic, neutrophilic and moderately halophilic
381 (Supplementary Table S2). Cells are non-motile. Gram-staining reaction is negative.
382 The phylogenetic position is in the family Sulfochloroflexaceae, order
383 Sulfochloroflexales, class Sulfochloroflexia of the phylum Chloroflexi. The type
384 species is *Sulfochloroflexus methaneseepsis*.

385 *Sulfochloroflexus methaneseepsis* (me.th.ane'seep.sis. L. gen. pl. n.
386 *methaneseepsis* of the deep-sea methane seeps). Cells are generally more than 20 µm
387 long and 0.5-0.6 µm wide, filamentous, facultatively anaerobic and have no flagellum.
388 From the sole carbon source utilization test, growth is stimulated by arabinose,
389 fructose, glucose, galactose, mannose, ribose, fumarate, pyruvate and peptone.
390 Growing at pH values of 6.0-8.0 (optimum, pH 7.0). The temperature range for
391 growth is 28-32 °C with an optimum at 28 °C. Growth occurs at NaCl concentrations
392 between 0.0-5.0% with optimum growth at 3.0% NaCl. Containing significant
393 proportions (>10 %) of the cellular fatty acids C_{16:0}, C_{15:0}2-OH, C_{17:1}ω6c and C_{18:1}ω7c.

394 The type strain, ZRK33^T, was isolated from the sediment of deep-sea cold seep, P.R.
395 China. The DNA G+C content of the type strain is 52.76%.

396 The detailed descriptions of other levels of Sulfochloroflexia were shown in the
397 Supplementary information.

398 ***S. methaneseepsis* ZRK33 assimilates sulfate and thiosulfate for growth**

399 Given that strain ZRK33 had a complete set genes of assimilatory sulfate reduction
400 and it was isolated from the deep-sea cold seep where is rich of different
401 sulfur-containing compounds [25,26], thus, we tested the effects of different
402 sulfur-containing inorganic substances (including Na₂SO₄, Na₂SO₃, Na₂S₂O₃, Na₂S)
403 on the growth of *S. methaneseepsis* ZRK33. The results showed that the supplement
404 of high concentration (200 mM) of Na₂SO₄ and Na₂S₂O₃ could significantly promote
405 the growth of strain ZRK33 (Figs. 5A and B). While low concentration of Na₂SO₄ and
406 Na₂S₂O₃ (20 mM) had no evident effects on the growth of strain ZRK33
407 (Supplementary Fig. S4), indicating this bacterium is only sensitive to high
408 concentrations of Na₂SO₄ and Na₂S₂O₃. Meanwhile, it is noting that the
409 concentrations of Na₂SO₄ and Na₂S₂O₃ were respectively decreased from 200 mM to
410 120 mM and 140 mM along with the growth of strain ZRK33 for 12 d, suggesting that
411 strain ZRK33 could effectively metabolize Na₂SO₄ and Na₂S₂O₃ (Figs. 5A and B).
412 Moreover, the average length of filamentous cells of strain ZRK33 became apparently
413 longer in the medium supplemented with 200 mM Na₂SO₄ (Fig. 5D) or Na₂S₂O₃ (Fig.
414 5E) than that in the control group (Fig. 5C), strongly suggesting that ZRK33 could

415 assimilate Na_2SO_4 and $\text{Na}_2\text{S}_2\text{O}_3$ and thereby generating extra energy for growth. In
416 comparison, the supplement of very low concentration (1 mM) of Na_2SO_3 and Na_2S
417 inhibited the growth of strain ZRK33 (Supplementary Fig. S4), indicating that SO_3^{2-}
418 and S^{2-} were harmful sulfur-containing compounds against the growth of strain
419 ZRK33.

420 **Proteomic analyses of sulfur metabolism in *S. methaneseepsis* ZRK33**

421 To better describe the sulfur metabolism of *S. methaneseepsis* ZRK33, we performed
422 the proteomic analysis of strain ZRK33 that cultured in the medium amended with or
423 without $\text{Na}_2\text{SO}_4/\text{Na}_2\text{S}_2\text{O}_3$ to explore the underlying mechanism of growth promotion,
424 given that ZRK33 could effectively assimilate $\text{Na}_2\text{SO}_4/\text{Na}_2\text{S}_2\text{O}_3$ for its growth. The
425 results showed that the expression of sulfurtransferase (TST), sulfatase-like hydrolase
426 and cysteine desulfurase-like protein were obviously up-regulation compared with the
427 control group, which were associated with sulfur metabolism (Fig. 6A). In particular,
428 TST is a key enzyme catalyzing $\text{S}_2\text{O}_3^{2-}$ to SO_3^{2-} and thereby joining into sulfur
429 assimilation (Fig. 3B), and it was significantly up-regulated in the presence of high
430 concentrations of $\text{Na}_2\text{SO}_4/\text{Na}_2\text{S}_2\text{O}_3$, especially $\text{Na}_2\text{S}_2\text{O}_3$. Surprisingly, the expressions
431 of other proteins associated with assimilatory sulfate reduction were not significantly
432 up-regulated in experimental groups, partly due to the single sampling time point that
433 might miss the exact time to detect the up-regulation of key proteins associated with
434 sulfur metabolism. Alternatively, the expressions of many proteins associated with
435 organic matter metabolisms toward energy production were evidently up-regulated,

436 including amino acids and sugar ABC transporters (Fig. 6B),
437 saccharides/peptides/amino acids degradation (Fig. 6C), and energy production (Fig.
438 6D). Correspondingly, the expressions of almost all genes involved in EMP glycolysis
439 were also significantly up-regulated (Supplementary Figures S5). Thus, we speculated
440 that metabolization of sulfate and thiosulfate by strain ZRK33 may accelerate the
441 hydrolysis and uptake of saccharides and other organic matter and thereby
442 synthesizing energy to promote the growth [48]. Combining the results of catalyzing
443 of sulfate and thiosulfate to other formations (Figs. 5C and 5D), we believe that strain
444 ZRK33 possesses a capability to assimilate inorganic sulfur-containing compounds
445 (e.g. sulfate and thiosulfate) that ubiquitously existing in the deep-sea environments
446 and thereby contributing to the deep-sea sulfur cycling to some extent.

447 Based on the combination of proteomic, genomic and physiological
448 characteristics, we propose a model towards central metabolic traits of strain ZRK33
449 (Fig. 7). In this model, central metabolisms including EMP glycolysis, oxidative
450 pentose phosphate pathway, TCA cycle (tricarboxylic acid cycle), assimilatory sulfate
451 reduction, urea cycle and electron transport system are shown. All the above items are
452 closely related to the energy production in strain ZRK33. Briefly, strain ZRK33
453 contains a number of genes related to ABC transporters of amino acids, peptides and
454 sugar, which could transport these organic matters into the cell to participate in EMP
455 glycolysis and oxidative pentose phosphate pathway. These processes eventually
456 drive the formation of pyruvate and acetyl-CoA, which enter the TCA cycle to

457 produce energy for the growth of strain ZRK33. Of note, sulfate and thiosulfate could
458 be converted to cysteine and thereby entering the pyruvate synthesis pathway through
459 the assimilatory sulfate reduction, which might promote the saccharides degradation
460 and utilization via some unknown mechanisms. Moreover, strain ZRK33 could fix
461 nitrogen and carbon dioxide to involve in the urea cycle, and corresponding
462 metabolites can join into the TCA cycle for energy generation. Meanwhile, the F-type
463 ATP synthase, cytochrome bd ubiquinol oxidase and H⁺-transporting NADH:
464 Quinone oxidoreductase required for energy production are also present in the
465 genome of strain ZRK33. Overall, *S. methaneseepsis* ZRK33 is a representative of a
466 novel clade of the phylum Chloroflexi that possessing diverse metabolic pathways for
467 energy production, providing an evidence that Chloroflexi members are a group of
468 high-abundance bacteria ubiquitously distributed in different environments.

469 **Wide distribution of assimilatory and dissimilatory sulfate reduction pathways in**
470 **the deep-sea Chloroflexi bacteria**

471 To evaluate the contribution of Chloroflexi bacteria to the deep-sea sulfur cycling, we
472 further analyzed the distribution of genes encoding key enzymes responsible for both
473 assimilatory (Fig. 8A) and dissimilatory (Fig. 8B) sulfate reduction in 27
474 metagenome-assembled genomes (MAGs) of Chloroflexi bacteria derived from both
475 deep-sea cold seep and hydrothermal vents sediments. Through a thorough analysis of
476 27 MAGs, we found that diverse genes encoding key enzymes in charge of
477 assimilatory and dissimilatory sulfate reduction, including adenylyl-sulfate kinase

478 (CysC), 3', 5'-bisphosphate nucleotidase (CysQ), sulfate adenylyltransferase (CysN),
479 anaerobic sulfite reductase (AsrA, AsrB and AsrC) and dissimilatory sulfite reductase
480 (DsrA and DsrB), were widely distributed in both cold seep and hydrothermal vents
481 derived MAGs (Fig. 8C). Of note, genes encoding AsrA and AsrB were present in
482 most MAGs, however, genes encoding DsrA and DsrB only broadly existed in the
483 hydrothermal vents-derived MAGs (Fig. 8C). DsrA and DsrB are typical symbols of
484 microbes mediating dissimilatory sulfate reduction [4]. Therefore, we propose
485 dissimilatory sulfate reduction might be often adopted by the members of Chloroflexi
486 in the hydrothermal vents. Nonetheless, Chloroflexi bacteria should be important
487 participants in sulfur cycling in the deep-sea environments, given their high
488 abundance in both cold seep and hydrothermal vents.

489 **Discussion**

490 Microorganisms in the deep marine subsurface sediments represent a large unexplored
491 biosphere, exploring and resolving their metabolisms are essential to understand the
492 global biogeochemical cycles [59-61]. Despite the global importance of these
493 microorganisms, deep-sea sediments are among the least understood environments,
494 partly due to the difficulty of sampling as well as the complexity of inhabiting
495 communities [59]. With this, the majority of deep-sea microbial diversity remains
496 uncultured, hampering a more thorough understanding of their unique biology
497 [3,59,62]. One of the striking characteristics of these uncultured lineages is that most
498 of them are dominant population, for example, the large proportion of uncultured

499 microbes was estimated to make up more than 75% of sediment genera [63].
500 Therefore, it is crucial to increase our capability for bringing microorganisms from
501 the environment into culture [60], which will advance our understanding of their
502 global biogeochemical cycles [48]. Among the uncultured majorities, the phylum
503 Chloroflexi is ubiquitous and often abundant in sediments, soils and wastewater
504 treatment systems, as well as in deep-sea extreme environments [64].

505 Indeed, our OTUs sequencing results clearly show that the abundance of the
506 phylum Chloroflexi is both the second most in the domain Bacteria that living in the
507 cold seep and hydrothermal vents sediments (Figs. 1A and 1B). Although Chloroflexi
508 bacteria are widespread on Earth, the puzzling thing is the extreme difficulty to
509 culture Chloroflexi members from various environments, leading to a poor
510 understanding with regard to their unique metabolisms that endowing them with
511 tremendous vitality. Therefore, it is an urgent need to obtain more uncultivated
512 isolates for better resolving their diversity and ecological roles, especially from the
513 deep-sea environments given their potentials to participate in sulfur cycling [4,28].
514 When we looked through the previously reported characteristics of Chloroflexi
515 isolates, one of the striking features attracted our attention: most cultured Chloroflexi
516 could tolerate a high concentration of rifampicin (50 $\mu\text{g}/\text{mL}$) [13,23]. It is known that
517 rifampicin is an effective inhibitor of DNA-dependent RNA polymerase and inhibits
518 the growth of many bacteria [23]. Therefore, in the present study, we developed an
519 effective enrichment method by keeping a constant rifampicin pressure in the

520 enrichment and isolation medium (Fig. 2A). Indeed, we successfully obtained a novel
521 Chloroflexi isolate, strain ZRK33, from the cold seep samples (Fig. 2). Strikingly,
522 strain ZRK33 possessed a very fast growth rate (4 h for doubling time) compared to
523 other reported Chloroflexi isolates (6 h to 19 days for doubling time) (Supplementary
524 Table S2), providing a great advantage for us to promptly perform various assays.
525 Overall, we strongly recommend the researchers to use rifampicin as a selection
526 pressure to enrich and culture novel isolates of Chloroflexi in the future.

527 Additionally, we proposed strain ZRK33 as a representative of a novel class of
528 the phylum Chloroflexi. The reasons are as following: (1) strain ZRK33 showed only
529 ~82% 16S rRNA gene identity with other cultured isolates, which meets the proposed
530 thresholds for median (86.35%) and minimum (80.38%) sequence identity values to
531 build a novel class [58]; (2) the phylogenetic analyses based on the genome
532 (Supplementary Figure S1), beta RpoB (Supplementary Figure S2) and EF-Tu
533 (Supplementary Figure S3) all support the classification of strain ZRK33 as the type
534 strain of a new class; (3) strain ZRK33 is facultatively anaerobic, however, the
535 Anaerolineae class bacteria are obligately anaerobic (Supplementary Table S2)[13],
536 even though the novel clade shows the highest identity with the Anaerolineae class.
537 Taken together, we propose strain ZRK33 together with *Aggregatilinea lenta*
538 MO-CFX2^T to represent a novel class of Chloroflexi phylum, though strain
539 MO-CFX2^T was thought to be a representative of a novel order of the class
540 Anaerolineae [13].

541 Notably, we find that strain ZRK33 contains a complete set of genes associated
542 with assimilatory sulfate reduction (Fig. 3B), providing potentials to involve into
543 sulfur cycling. Therefore, we name this novel isolate as *Sulfochloroflexus*
544 *methaneseepsis* ZRK33, which belonging to Sulfochloroflexia classis nov.,
545 Sulfochloroflexales ord. nov., Sulfochloroflexaceae fam. nov.. The cycling of sulfur is
546 a dominant metabolism pathway for the marine subsurface microorganisms [26,65],
547 and deep-sea Chloroflexi bacteria were predicted to respire oxidized sulfur
548 compounds [4] and metabolize multiple organosulfur compounds [28] based on
549 metagenomics data. However, to date, no studies based on the pure culture have
550 verified that Chloroflexi members indeed drive sulfur cycling of deep-sea
551 environments. Take advantage of pure cultivation of *S. methaneseepsis* ZRK33, we
552 verified its actual involvement of both sulfate and thiosulfate assimilatory processes
553 (Fig. 5), and the sulfur assimilatory greatly facilitates the growth and morphogenesis
554 of ZRK33 via promoting the transport and metabolization of saccharides and other
555 organic matter (Fig. 6). However, strain ZRK33 only responds to high concentrations
556 of sulfate and thiosulfate (200 mM), given the high concentrations of different
557 sulfur-containing compounds [25,26] existing in the cold seep and some microbes
558 possessing a capability to enrich sulfur-containing compounds (such as elemental
559 sulfur and polysulfide [26,66]), we speculate this phenomenon is possible to happen
560 in the deep-sea cold seep sediments.

561 Most importantly, large portion of the genes associated with assimilatory or
562 dissimilatory sulfate reduction are widely distributed in the Chloroflexi MAGs
563 derived from deep-sea cold seep and hydrothermal vents (Fig. 8), which strongly
564 suggesting Chloroflexi bacteria are key players in the sulfur cycling of deep biosphere.
565 In combination with the reports that the other two Chloroflexi lineages (SAR202
566 group and Dehalococcoidia class) possessing potentials to drive sulfur
567 metabolizations, it is reasonable to affirm the phylum Chloroflexi greatly contributes
568 to the ocean sulfur cycling. Actually, we tried to check the metabolisms of strain
569 ZRK33 that cultured in the deep-sea cold seep as performed previously [48],
570 unfortunately, the cells of strain ZRK33 were invaded by some unknown microbes
571 that leading the failure of *in situ* test toward its involvement of sulfur cycling. We are
572 improving the experimental apparatus and procedure, which will greatly benefit us to
573 check the central metabolisms of strain ZRK33 *in situ* in the near future.

574 **Acknowledgements**

575 This work was funded by the Major Research Plan of the National Natural Science
576 Foundation (Grant No. 92051107), China Ocean Mineral Resources R&D Association
577 Grant (Grant No. DY135-B2-14), Key Deployment Projects of Center of Ocean
578 Mega-Science of the Chinese Academy of Sciences (Grant No. COMS2020Q04),
579 Strategic Priority Research Program of the Chinese Academy of Sciences (Grant No.
580 XDA22050301), National Key R and D Program of China (Grant No.
581 2018YFC0310800), the Taishan Young Scholar Program of Shandong Province

582 (tsqn20161051), and Qingdao Innovation Leadership Program (Grant No.
583 18-1-2-7-zhc) for Chaomin Sun. This study is also funded by the Open Research
584 Project of National Major Science & Technology Infrastructure (*RV KEXUE*) (Grant
585 No. NMSTI-KEXUE2017K01).

586 **Author contributions**

587 RZ and CS conceived and designed the study; RZ conducted most of the experiments;
588 RL, YS and GL collected the samples from the deep-sea cold seep; RC helped to
589 analyze the metagenomes; RZ and CS lead the writing of the manuscript; all authors
590 contributed to and reviewed the manuscript.

591 **Conflict of interest**

592 The authors declare that there are no any competing financial interests in relation to
593 the work described.

594 **References**

- 595 1. Kallmeyer J, Pockalny R, Adhikari RR, Smith DC, D'Hondt S. Global distribution
596 of microbial abundance and biomass in subseafloor sediment. *P Natl Acad Sci USA*.
597 (2012); 109: 16213-16216.
- 598 2. Parkes RJ, Cragg BA, Wellsbury P. Recent studies on bacterial populations and
599 processes in subseafloor sediments: A review. *Hydrogeol J*. (2002); 10: 346-346.
- 600 3. Inagaki F, Nunoura T, Nakagawa S, Teske A, Lever M, Lauer A, et al. Biogeographical
601 distribution and diversity of microbes in methane hydrate-bearing deep marine sediments,
602 on the Pacific Ocean Margin. *P Natl Acad Sci USA*. (2006); 103: 2815-2820.
- 603 4. Wasmund K, Cooper M, Schreiber L, Lloyd KG, Baker BJ, Petersen DG, et al.
604 Single-cell genome and group-specific *dsrAB* sequencing implicate marine members of
605 the class Dehalococcoidia (Phylum Chloroflexi) in sulfur cycling. *mBio*. (2016); 7.
- 606 5. Biddle JF, Fitz-Gibbon S, Schuster SC, Brenchley JE, House CH. Metagenomic
607 signatures of the Peru Margin subseafloor biosphere show a genetically distinct
608 environment. *P Natl Acad Sci USA*. (2008); 105: 10583-10588.

- 609 6. Blazejak A, Schippers A. High abundance of JS-1-and Chloroflexi-related Bacteria in
610 deeply buried marine sediments revealed by quantitative, real-time PCR. FEMS
611 Microbiol Ecol. (2010); 72: 198-207.
- 612 7. Parkes RJ, Cragg B, Roussel E, Webster G, Weightman A, Sass H. A review of
613 prokaryotic populations and processes in sub-seafloor sediments, including
614 biosphere:geosphere interactions. Mar Geol. (2014); 352: 409-425.
- 615 8. Fry JC, Parkes RJ, Cragg BA, Weightman AJ, Webster G. Prokaryotic biodiversity
616 and activity in the deep subseafloor biosphere. FEMS Microbiol Ecol. (2008); 66:
617 181-196.
- 618 9. Speirs LBM, Rice DTF, Petrovski S, Seviour RJ. The phylogeny, biodiversity, and
619 ecology of the Chloroflexi in activated sludge. Front Microbiol. (2019); 10.
- 620 10. Bovio P, Cabezas A, Etchebehere C. Preliminary analysis of Chloroflexi populations in
621 full-scale UASB methanogenic reactors. J Appl Microbiol. (2019); 126: 667-683.
- 622 11. Schmitt S, Deines P, Behnam F, Wagner M, Taylor MW. Chloroflexi bacteria are
623 more diverse, abundant, and similar in high than in low microbial abundance sponges.
624 FEMS Microbiol Ecol. (2011); 78: 497-510.
- 625 12. Sorokin DY, Lucker S, Vejmekova D, Kostrikina NA, Kleerebezem R, Rijpstra WIC, et
626 al. Nitrification expanded: discovery, physiology and genomics of a nitrite-oxidizing
627 bacterium from the phylum Chloroflexi. ISME J. (2012); 6: 2245-2256.
- 628 13. Nakahara N, Nobu MK, Takaki Y, Miyazaki M, Tasumi E, Sakai S, et al. *Aggregatilinea*
629 *lenta* gen. nov., sp. nov., a slow-growing, facultatively anaerobic bacterium isolated from
630 subseafloor sediment, and proposal of the new order Aggregatilineales ord. nov. within
631 the class Anaerolineae of the phylum Chloroflexi. Int J Syst Evol Micr. (2019); 69:
632 1185-1194.
- 633 14. Gupta RS, Chander P, George S. Phylogenetic framework and molecular signatures for
634 the class Chloroflexi and its different clades; proposal for division of the class Chloroflexi
635 class. nov into the suborder Chloroflexineae subord. nov., consisting of the emended
636 family Oscillochloridaceae and the family Chloroflexaceae fam. nov., and the suborder
637 Roseiflexineae subord. nov., containing the family Roseiflexaceae fam. nov. Anton
638 Leeuw Int J G. (2013); 103: 99-119.
- 639 15. Yamada T, Sekiguchi Y, Hanada S, Imachi H, Ohashi A, Harada H, et al. *Anaerolinea*
640 *thermolimosa* sp nov., *Levilinea saccharolytica* gen. nov., sp nov and *Leptolinea*
641 *tardivitalis* gen. nov., so. nov., novel filamentous anaerobes, and description of the new
642 classes anaerolineae classis nov and Caldilineae classis nov in the bacterial phylum
643 Chloroflexi. Int J Syst Evol Micr. (2006); 56: 1331-1340.
- 644 16. Yabe S, Aiba Y, Sakai Y, Hazaka M, Yokota A. *Thermosporothrix hazakensis* gen.
645 nov., sp nov., isolated from compost, description of Thermosporotrichaceae fam. nov
646 within the class Ktedonobacteria Cavaletti et al. 2007 and emended description of the
647 class Ktedonobacteria. Int J Syst Evol Micr. (2010); 60: 1794-1801.
- 648 17. Garrity GM, Holt JG, Perry JJ. (2001) In Boone, D. R., Castenholz, R. W. and Garrity,
649 G. M. (eds.), *Bergey's Manual® of Systematic Bacteriology: Volume One : The Archaea*

- 650 *and the Deeply Branching and Phototrophic Bacteria*. Springer New York, New York,
651 NY, pp. 447-450.
- 652 18. Löffler FE, Yan J, Ritalahti KM, Adrian L, Edwards EA, Konstantinidis KT, et al.
653 *Dehalococcoides mccartyi* gen. nov., sp nov., obligately organohalide-respiring anaerobic
654 bacteria relevant to halogen cycling and bioremediation, belong to a novel bacterial class,
655 Dehalococcoidia classis nov., order Dehalococcoidales ord. nov and family
656 Dehalococcoidaceae fam. nov., within the phylum Chloroflexi. *Int J Syst Evol Micr.*
657 (2013); 63: 625-635.
- 658 19. Kochetkova TV, Zayulina KS, Zhigarkov VS, Minaev NV, Chichkov BN, Novikov AA,
659 et al. *Tepidiforma bonchosmolovskayae* gen. nov., sp. nov., a moderately thermophilic
660 Chloroflexi bacterium from a Chukotka hot spring (Arctic, Russia), representing a novel
661 class, Tepidiformia, which includes the previously uncultivated lineage OLB14. *Int J Syst*
662 *Evol Micr.* (2020); 70: 1192-1202.
- 663 20. Dodsworth JA, Gevorkian J, Despujos F, Cole JK, Murugapiran SK, Ming H, et al.
664 *Thermoflexus hugenholtzii* gen. nov., sp. nov., a thermophilic, microaerophilic,
665 filamentous bacterium representing a novel class in the Chloroflexi, *Thermoflexia classis*
666 nov., and description of Thermoflexaceae fam. nov. and Thermoflexales ord. nov. . *Int J*
667 *Syst Evol Micr.* (2014); 64: 3331-3331.
- 668 21. Kawaiichi S, Ito N, Kamikawa R, Sugawara T, Yoshida T, Sako Y. *Ardenticatena*
669 *maritima* gen. nov., sp nov., a ferric iron- and nitrate-reducing bacterium of the phylum
670 'Chloroflexi' isolated from an iron-rich coastal hydrothermal field, and description of
671 *Ardenticatena classis nov.* *Int J Syst Evol Micr.* (2013); 63: 2992-3002.
- 672 22. Rappe MS, Giovannoni SJ. The uncultured microbial majority. *Annu Rev Microbiol.*
673 (2003); 57: 369-394.
- 674 23. Imachi H, Sakai S, Lipp JS, Miyazaki M, Saito Y, Yamanaka Y, et al. *Pelolinea*
675 *submarina* gen. nov., sp nov., an anaerobic, filamentous bacterium of the phylum
676 Chloroflexi isolated from subseafloor sediment. *Int J Syst Evol Micr.* (2014); 64:
677 812-818.
- 678 24. Imachi H, Aoi K, Tasumi E, Saito Y, Yamanaka Y, Saito Y, et al. Cultivation of
679 methanogenic community from subseafloor sediments using a continuous-flow bioreactor.
680 *ISME J.* (2011); 5: 1913-1925.
- 681 25. Wasmund K, Mussmann M, Loy A. The life sulfuric: microbial ecology of sulfur
682 cycling in marine sediments. *Env Microbiol Rep.* (2017); 9: 323-344.
- 683 26. Zhang J, Liu R, Xi SC, Cai RN, Zhang X, Sun CM. A novel bacterial thiosulfate
684 oxidation pathway provides a new clue about the formation of zero-valent sulfur in deep
685 sea. *ISME J.* (2020); 14: 2261-2274.
- 686 27. Fullerton H, Moyer CL. Comparative single-cell genomics of Chloroflexi from the
687 Okinawa Trough deep-subsurface biosphere. *Appl Environ Microb.* (2016); 82:
688 3000-3008.
- 689 28. Mehrshad M, Rodriguez-Valera F, Amoozegar MA, Lopez-Garcia P, Ghai R. The
690 enigmatic SAR202 cluster up close: shedding light on a globally distributed dark ocean
691 lineage involved in sulfur cycling. *ISME J.* (2018); 12: 655-668.

- 692 29. Murray MG, Thompson WF. Rapid isolation of high molecular-weight plant DNA.
693 Nucleic Acids Res. (1980); 8: 4321-4325.
- 694 30. Magoc T, Salzberg SL. FLASH: fast length adjustment of short reads to improve genome
695 assemblies. Bioinformatics. (2011); 27: 2957-2963.
- 696 31. Bokulich NA, Subramanian S, Faith JJ, Gevers D, Gordon JI, Knight R, et al.
697 Quality-filtering vastly improves diversity estimates from Illumina amplicon sequencing.
698 Nat Methods. (2013); 10: 57-U11.
- 699 32. Edgar RC, Haas BJ, Clemente JC, Quince C, Knight R. UCHIME improves
700 sensitivity and speed of chimera detection. Bioinformatics. (2011); 27: 2194-2200.
- 701 33. Haas BJ, Gevers D, Earl AM, Feldgarden M, Ward DV, Giannoukos G, et al. Chimeric
702 16S rRNA sequence formation and detection in Sanger and 454-pyrosequenced PCR
703 amplicons. Genome Res. (2011); 21: 494-504.
- 704 34. Edgar RC. UPARSE: highly accurate OTU sequences from microbial amplicon reads.
705 Nat Methods. (2013); 10: 996-998.
- 706 35. Quast C, Pruesse E, Yilmaz P, Gerken J, Schweer T, Yarza P, et al. The SILVA
707 ribosomal RNA gene database project: improved data processing and web-based tools.
708 Nucleic Acids Res. (2013); 41: D590-D596.
- 709 36. Chen YX, Chen YS, Shi CM, Huang ZB, Zhang Y, Li SK, et al. SOAPnuke: a
710 MapReduce acceleration-supported software for integrated quality control and
711 preprocessing of high-throughput sequencing data. Gigascience. (2017); 7.
- 712 37. Li DH, Liu CM, Luo RB, Sadakane K, Lam TW. MEGAHIT: an ultra-fast
713 single-node solution for large and complex metagenomics assembly via succinct de
714 Bruijn graph. Bioinformatics. (2015); 31: 1674-1676.
- 715 38. Wu YW, Simmons BA, Singer SW. MaxBin 2.0: an automated binning algorithm to
716 recover genomes from multiple metagenomic datasets. Bioinformatics. (2016); 32:
717 605-607.
- 718 39. Kang DWD, Li F, Kirton E, Thomas A, Egan R, An H, et al. MetaBAT 2: an adaptive
719 binning algorithm for robust and efficient genome reconstruction from metagenome
720 assemblies. Peerj. (2019); 7.
- 721 40. Alneberg J, Bjarnason BS, de Bruijn I, Schirmer M, Quick J, Ijaz UZ, et al. Binning
722 metagenomic contigs by coverage and composition. Nat Methods. (2014); 11: 1144-1146.
- 723 41. Uritskiy GV, DiRuggiero J, Taylor J. MetaWRAP-a flexible pipeline for
724 genome-resolved metagenomic data analysis. Microbiome. (2018); 6.
- 725 42. Parks DH, Imelfort M, Skennerton CT, Hugenholtz P, Tyson GW. CheckM:
726 assessing the quality of microbial genomes recovered from isolates, single cells, and
727 metagenomes. Genome Res. (2015); 25: 1043-1055.
- 728 43. Dombrowski N, Teske AP, Baker BJ. Expansive microbial metabolic versatility and
729 biodiversity in dynamic Guaymas Basin hydrothermal sediments. Nat Commun. (2018);
730 9.
- 731 44. Fardeau ML, Ollivier B, Patel BKC, Magot M, Thomas P, Rimbault A, et al. *Thermotoga*
732 *hypogea* sp. nov., a xylanolytic, thermophilic bacterium from an oil-producing well. Int J
733 Syst Bacteriol. (1997); 47: 1013-1019.

- 734 45. Buchan A, LeClerc GR, Gulvik CA, Gonzalez JM. Master recyclers: features and
735 functions of bacteria associated with phytoplankton blooms. *Nat Rev Microbiol.* (2014);
736 12: 686-698.
- 737 46. Sekiguchi Y, Yamada T, Hanada S, Ohashi A, Harada H, Kamagata Y.
738 *Anaerolinea thermophila* gen. nov., sp nov and *Caldilinea aerophila* gen. nov., sp nov.,
739 novel filamentous thermophiles that represent a previously uncultured lineage of the
740 domain Bacteria at the subphylum level. *Int J Syst Evol Micr.* (2003); 53: 1843-1851.
- 741 47. Graham L, Orenstein JM. Processing tissue and cells for transmission electron
742 microscopy in diagnostic pathology and research. *Nat Protoc.* (2007); 2: 2439-2450.
- 743 48. Zheng RK, Liu R, Shan YQ, Cai RN, Liu G, Sun CM. Characterization of the first
744 cultured free-living representative of *Candidatus Izimaplasma* uncovers its unique
745 biology. *bioRxiv.* (2020).
- 746 49. Loman NJ, Quinlan AR. Poretools: a toolkit for analyzing nanopore sequence data.
747 *Bioinformatics.* (2014); 30: 3399-3401.
- 748 50. Koren S, Walenz BP, Berlin K, Miller JR, Bergman NH, Phillippy AM. Canu:
749 scalable and accurate long-read assembly via adaptive k-mer weighting and repeat
750 separation. *Genome Res.* (2017); 27: 722-736.
- 751 51. Richter M, Rossello-Mora R, Glockner FO, Peplies J. JSpeciesWS: a web server for
752 prokaryotic species circumscription based on pairwise genome comparison.
753 *Bioinformatics.* (2016); 32: 929-931.
- 754 52. Meier-Kolthoff JP, Auch AF, Klenk HP, Goker M. Genome sequence-based species
755 delimitation with confidence intervals and improved distance functions. *Bmc*
756 *Bioinformatics.* (2013); 14.
- 757 53. Wu DY, Jospin G, Eisen JA. Systematic identification of gene families for use as
758 "markers" for phylogenetic and phylogeny-driven ecological studies of Bacteria and
759 Archaea and their major subgroups. *Plos One.* (2013); 8.
- 760 54. Darling AE, Jospin G, Lowe E, Matsen FIV, Bik HM, Eisen JA. PhyloSift:
761 phylogenetic analysis of genomes and metagenomes. *Peerj.* (2014); 2.
- 762 55. Trifinopoulos J, Nguyen LT, von Haeseler A, Minh BQ. W-IQ-TREE: a fast online
763 phylogenetic tool for maximum likelihood analysis. *Nucleic Acids Res.* (2016); 44:
764 W232-W235.
- 765 56. Letunic I, Bork P. Interactive Tree Of Life (iTOL): an online tool for phylogenetic tree
766 display and annotation. *Bioinformatics.* (2007); 23: 127-128.
- 767 57. Letunic I, Bork P. Interactive tree of life (iTOL) v3: an online tool for the display and
768 annotation of phylogenetic and other trees. *Nucleic Acids Res.* (2016); 44: W242-W245.
- 769 58. Yilmaz P, Parfrey LW, Yarza P, Gerken J, Pruesse E, Quast C, et al. The SILVA and
770 "All-species Living Tree Project (LTP)" taxonomic frameworks. *Nucleic Acids Res.*
771 (2014); 42: D643-D648.
- 772 59. Baker BJ, Appller KE, Gong X. New microbial biodiversity in marine sediments. *Ann*
773 *Rev Mar Sci.* (2020).
- 774 60. Lewis WH, Tahon G, Geesink P, Sousa DZ, Ettema TJG. Innovations to culturing
775 the uncultured microbial majority. *Nat Rev Microbiol.* (2020).

- 776 61. Zheng RK, Sun CM. *Sphingosinithalassobacter tenebrarum* sp. nov., isolated from a
777 deep-sea cold seep. *Int J Syst Evol Micr.* (2020); 70: 5561-5566.
- 778 62. Henson MW, Lanclos VC, Faircloth BC, Thrash JC. Cultivation and genomics of the
779 first freshwater SAR11 (LD12) isolate. *ISME J.* (2018); 12: 1846-1860.
- 780 63. Lloyd KG, Steen AD, Ladau J, Yin J, Crosby L. Phylogenetically novel uncultured
781 microbial cells dominate Earth microbiomes. *mSystems.* (2018); 3.
- 782 64. Yamada T, Sekiguchi Y. Cultivation of Uncultured Chloroflexi Subphyla: Significance
783 and Ecophysiology of Formerly Uncultured Chloroflexi 'Subphylum I' with Natural and
784 Biotechnological Relevance. *Microbes Environ.* (2009); 24: 205-216.
- 785 65. D'Hondt S, Rutherford S, Spivack AJ. Metabolic activity of subsurface life in deep-sea
786 sediments. *Science.* (2002); 295: 2067-2070.
- 787 66. Xia Y, Lü C, Hou N, Xin Y, Liu J, Liu H, et al. Sulfide production and oxidation by
788 heterotrophic bacteria under aerobic conditions. *ISME J.* (2017); 11: 2754.

789

790

791

792

793

794

795

796

797

798

799

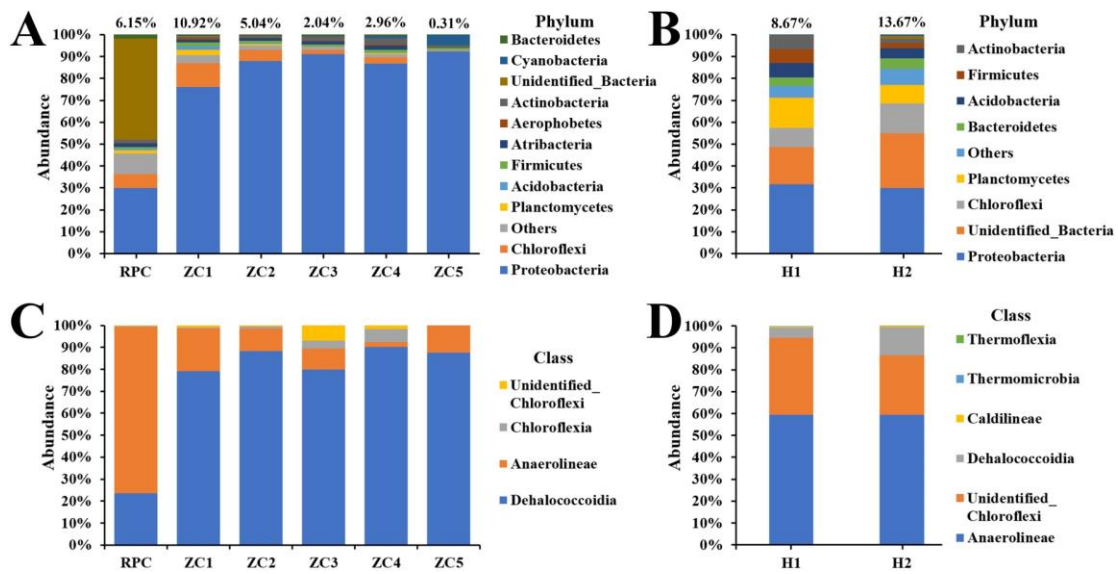
800

801

802

803

804 **Figure**



805

806 **Fig. 1.** Detection of the abundance of the phylum Chloroflexi derived from the
807 deep-sea cold seep and hydrothermal vents sediments. The community structure of six
808 sampling sites in the cold seep sediments and two sampling sites in the hydrothermal
809 vents sediments as revealed by 16S rRNA gene amplicon profiling. The relative
810 abundances of operational taxonomic units (OTUs) representing different bacteria are
811 shown at the phylum level (A and B) and class level (C and D). Panels A and C
812 represent samples from the cold seep; Panels B and D represent samples from the
813 hydrothermal vents.

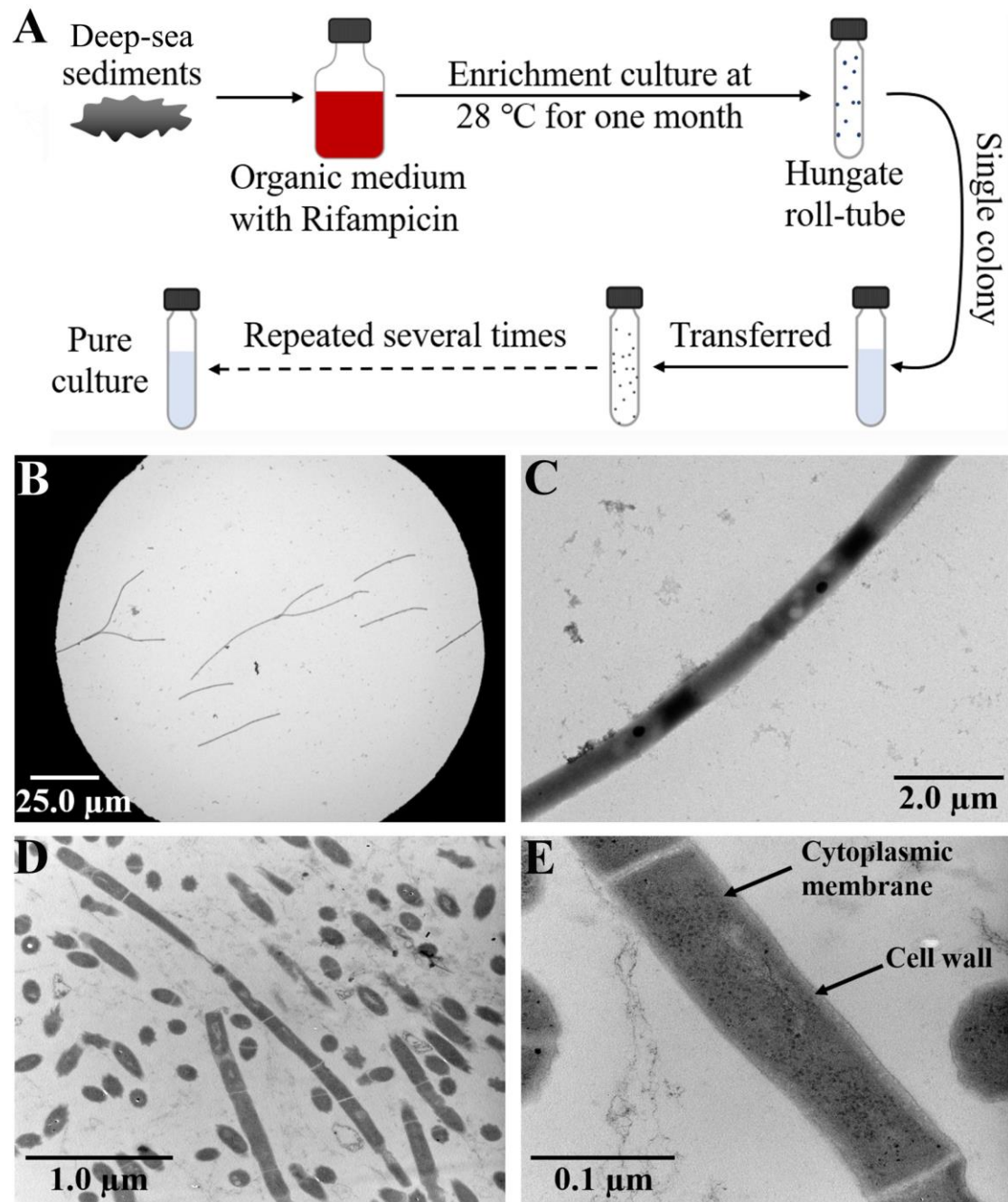
814

815

816

817

818



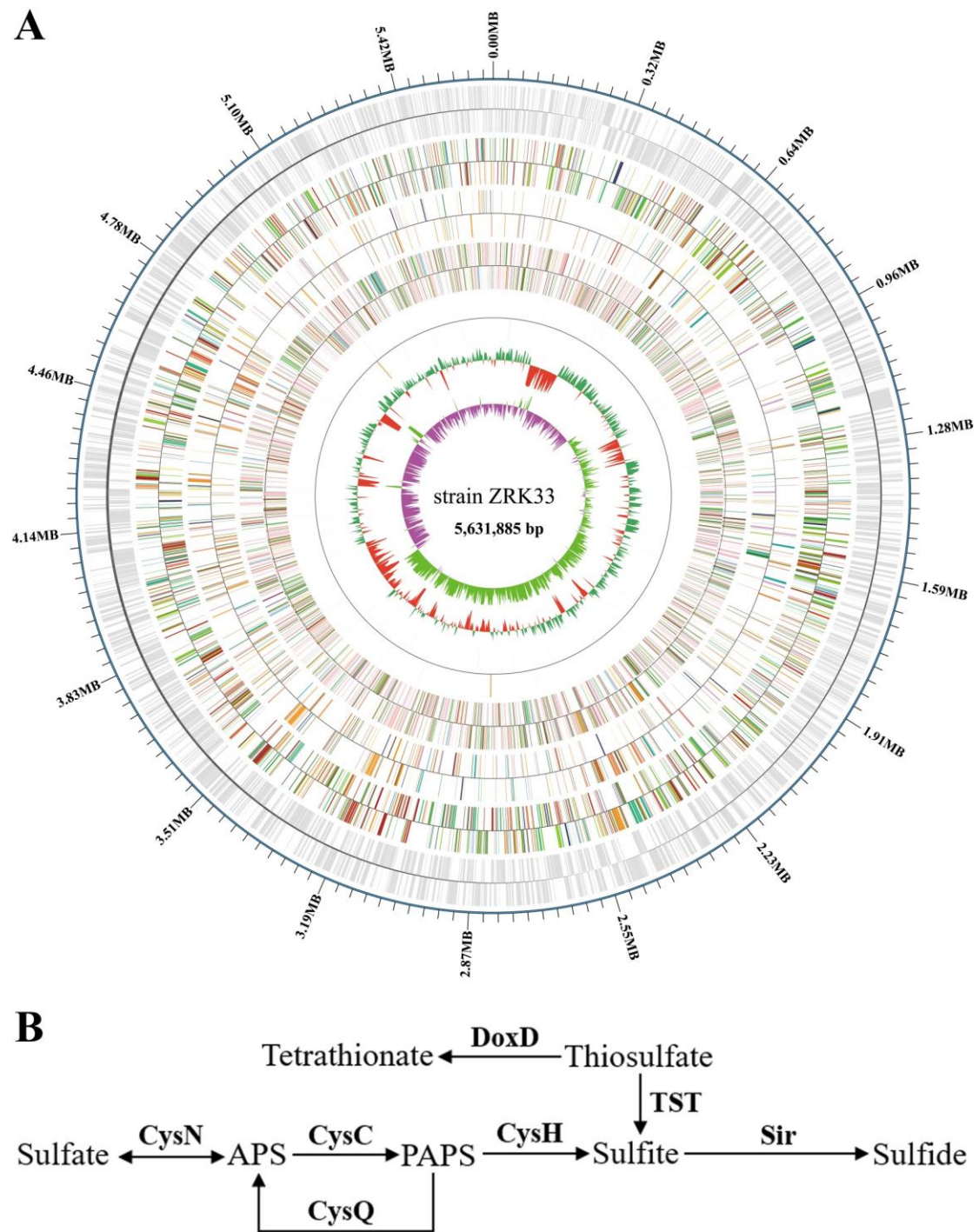
819

820 **Fig. 2.** Rifampicin resistance-driven enrichment and isolation strategy of Chloroflexi

821 bacteria. (A) Diagrammatic scheme of enrichment and isolation of Chloroflexi

822 bacteria. (B, C) TEM observation of strain ZRK33. (D, E) TEM observation of the

823 ultrathin sections of strain ZRK33.



824

825 **Fig. 3.** Genomic analysis of strain ZRK33. (A) Circular diagram of the genome of

826 strain ZRK33. Rings indicate, from outside to the center: a genome-wide marker with

827 a scale of 320 kb; forward strand genes, colored by COG category; reverse strand

828 genes, colored by COG category; gene function annotation (COG, KEGG, GO, NR,

829 CAZy, TCDB); RNA genes (tRNAs blue, rRNAs purple); GC content; GC skew. (B)

830 Proposed assimilatory sulfate reduction pathway identified in the genome of strain
831 ZRK33. Abbreviations: CysN, sulfate adenylyltransferase; Sat, sulfate
832 adenylyltransferase; CysC, adenylyl-sulfate kinase; CysQ, 3', 5'-bisphosphate
833 nucleotidase; CysH, phosphoadenosine phosphosulfate reductase; Sir, sulfite
834 reductase; TST, thiosulfate/3-mercaptopyruvate sulfurtransferase; DoxD, thiosulfate
835 dehydrogenase (quinone) large subunit; APS, adenosine 5'-phosphosulfate; PAPS,
836 3'-phosphoadenosine-5'-phosphosulfate (3'-phosphoadenylylsulfate).

837

838

839

840

841

842

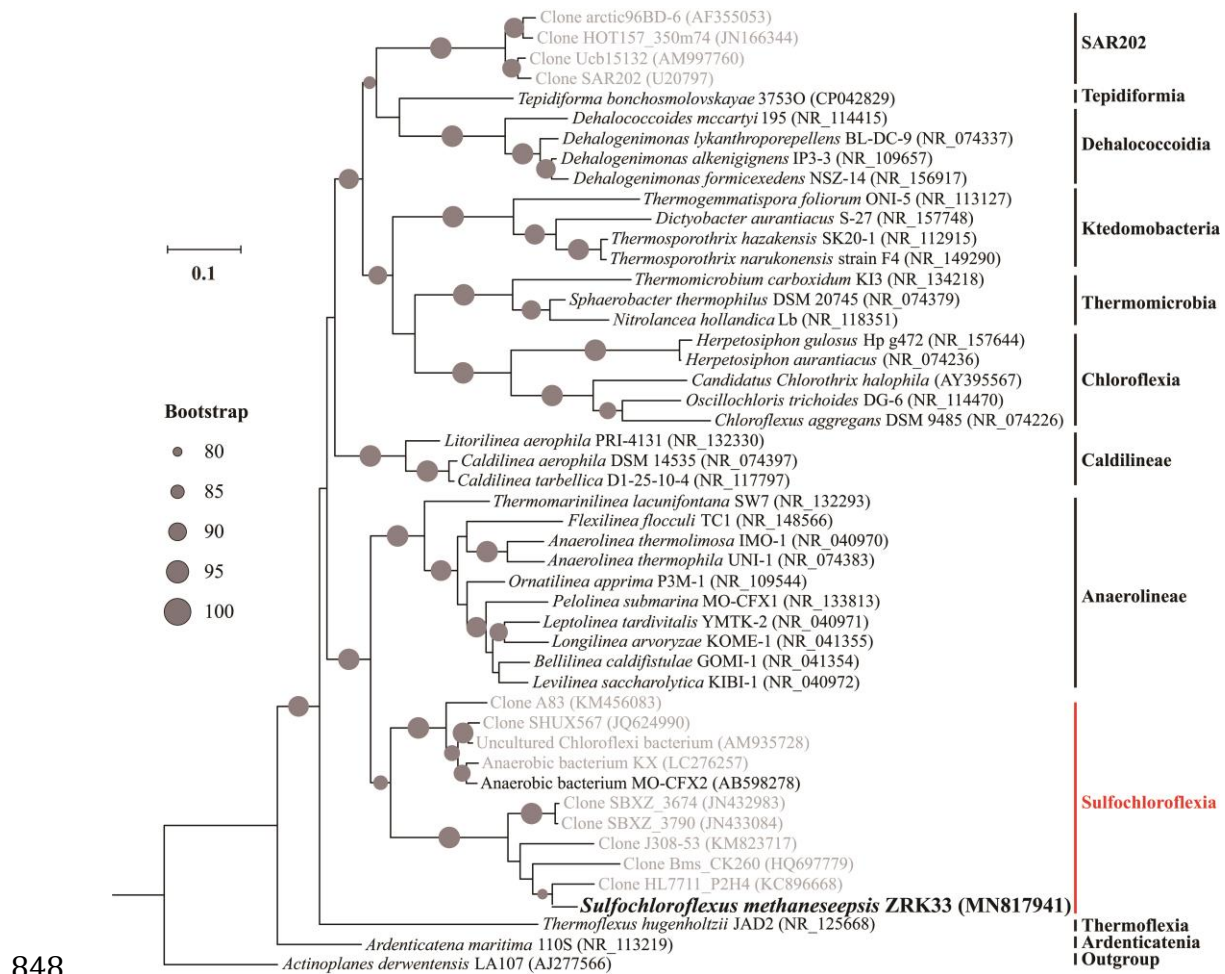
843

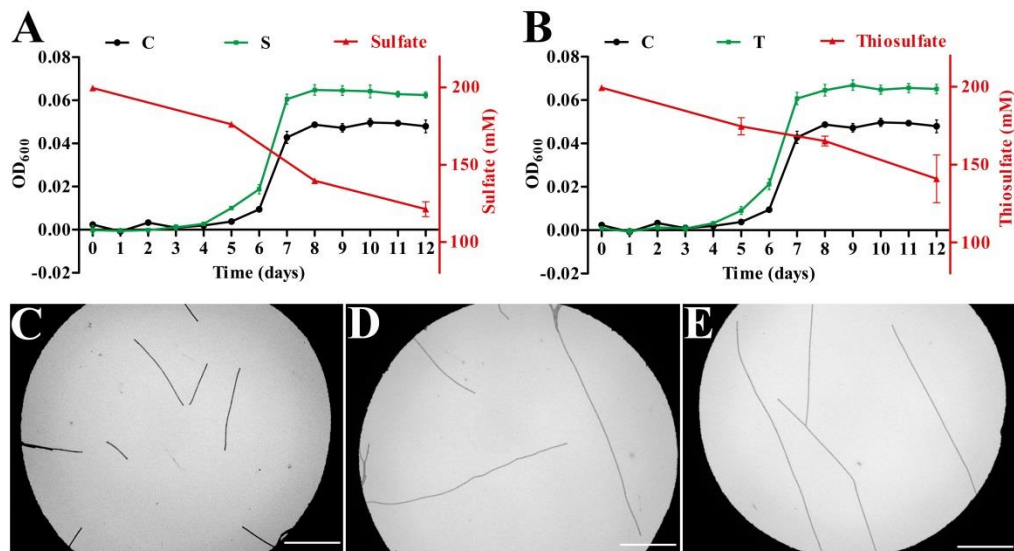
844

845

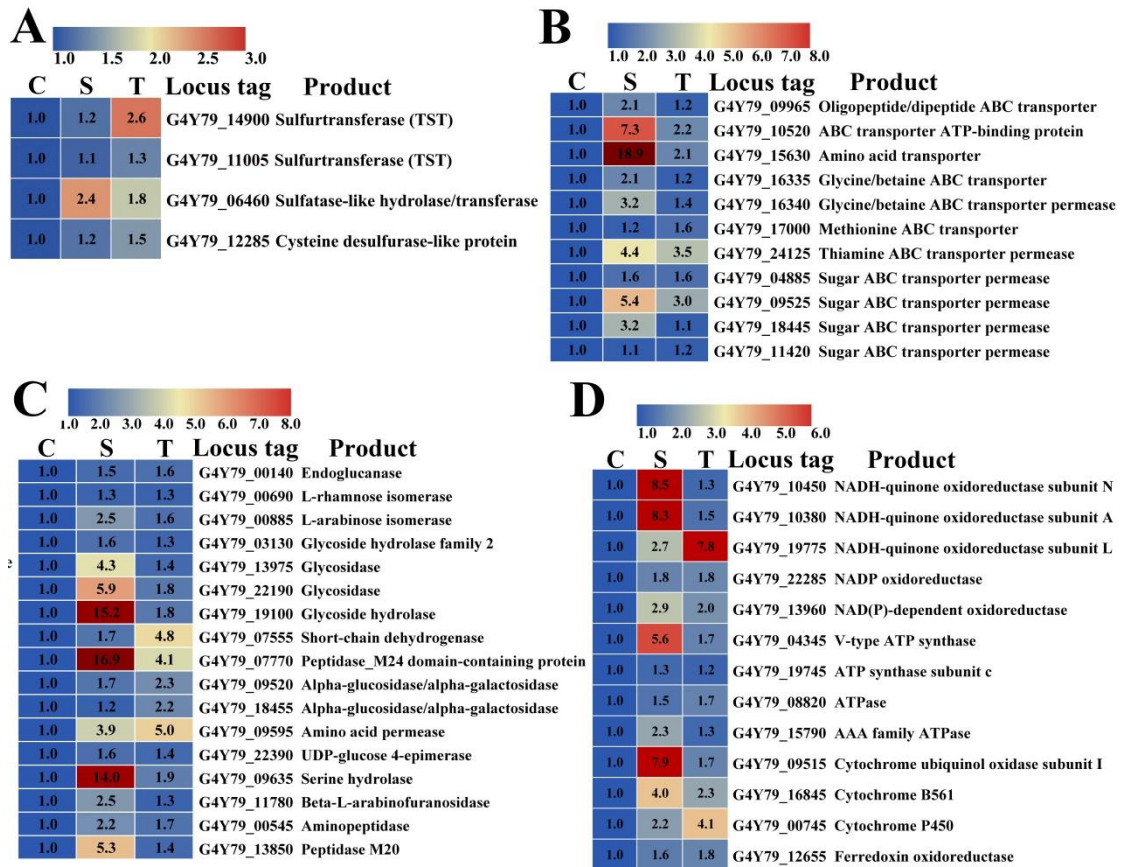
846

847

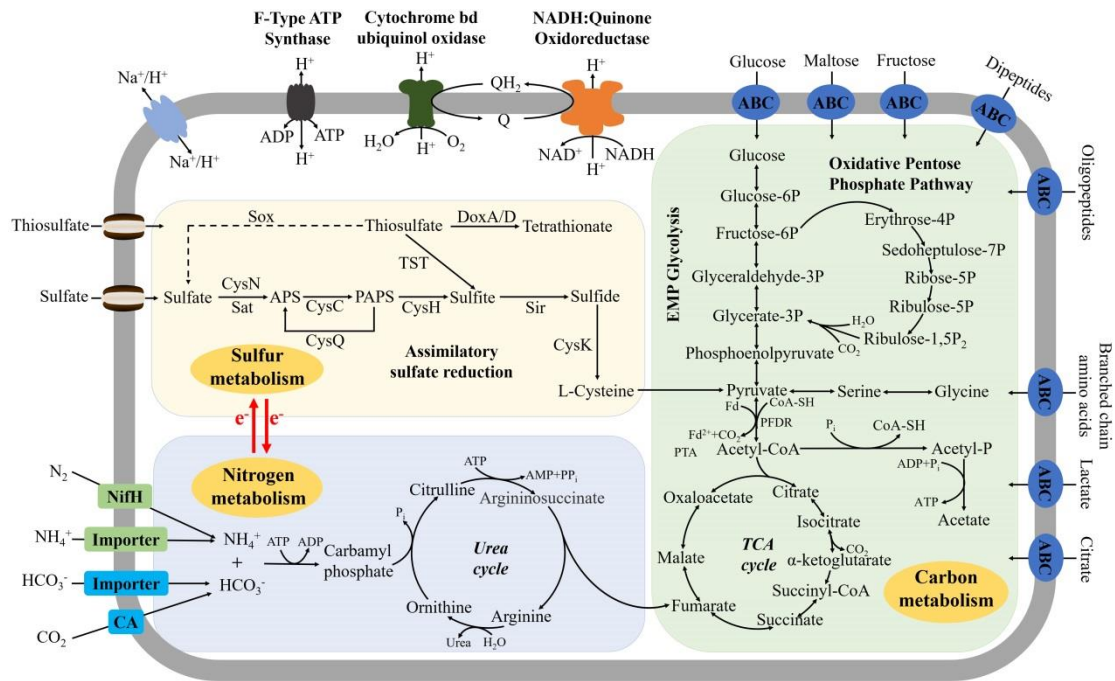




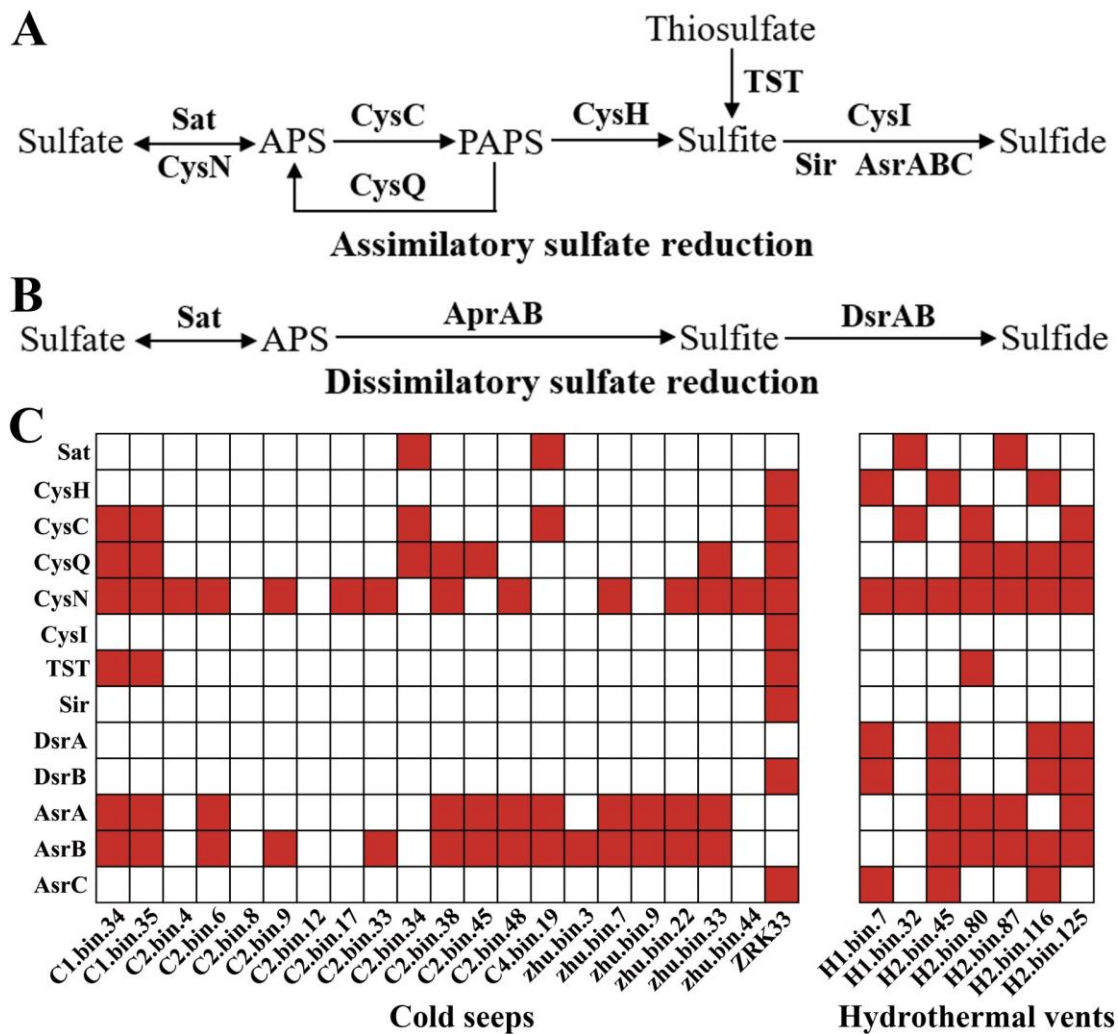
858 **Fig. 5.** Verification of sulfate and thiosulfate assimilation in *S. methaneseepsis*
859 ZRK33. (A) Growth assay and sulfate metabolization of strain ZRK33 cultured in the
860 medium supplemented without or with 200 mM Na₂SO₄. (B) Growth assay and
861 thiosulfate metabolization of strain ZRK33 cultured in the medium supplemented
862 without or with 200 mM Na₂S₂O₃. “C” indicates the control group, where strain
863 ZRK33 was cultured in the medium supplemented without extra Na₂SO₄ or Na₂S₂O₃;
864 “S” indicates the sulfate-treated group, where strain ZRK33 was cultured in the
865 medium supplemented with 200 mM Na₂SO₄; “T” indicates the thiosulfate-treated
866 group, where strain ZRK33 was cultured in the medium supplemented with 200 mM
867 Na₂S₂O₃. The black lines represent the growth curves of the control group; the green
868 lines represent the growth curves of experimental groups; the red lines represent the
869 variation tendency of concentrations of Na₂SO₄ or Na₂S₂O₃. (C) TEM observation of
870 strain ZRK33 that cultured in the ORG medium. (D) TEM observation of strain
871 ZRK33 that cultured in the ORG medium supplemented with 200 mM Na₂SO₄. (E)
872 TEM observation of strain ZRK33 that cultured in the ORG medium supplemented
873 with 200 mM Na₂S₂O₃. The bar is 20 μm in the panels C, D and E.



874 **Fig. 6.** Proteomic analysis of *S. methaneseepsis* ZRK33 cultured in the medium
 875 supplemented with sulfate and thiosulfate. (A) Proteomics based heat map showing all
 876 up-regulated proteins associated with sulfur metabolism. (B) Proteomics based heat
 877 map showing all up-regulated proteins associated with amino acids and sugar
 878 transporters. (C) Proteomics based heat map showing all up-regulated proteins
 879 associated with saccharides/amino acids/peptides hydrolases. (D) Proteomics based
 880 heat map showing all up-regulated proteins associated with energy production. “C”
 881 indicates the control group, where strain ZRK33 was cultured in the medium
 882 supplemented without extra Na_2SO_4 or $\text{Na}_2\text{S}_2\text{O}_3$; “S” indicates the sulfate-treated
 883 group, where strain ZRK33 was cultured in the medium supplemented with 200 mM
 884 Na_2SO_4 ; “T” indicates the thiosulfate-treated group, where strain ZRK33 was cultured
 885 in the medium supplemented 200 mM $\text{Na}_2\text{S}_2\text{O}_3$.



886 **Fig. 7.** Multi-omics based central metabolisms model of *S. methaneseepsis* ZRK33. In
 887 this model, three central metabolic pathways (associated with carbon, sulfur and
 888 nitrogen cyclings) including EMP glycolysis, oxidative pentose phosphate pathway,
 889 TCA cycle, urea cycle, assimilatory sulfate reduction and some electron transport
 890 systems are shown and highlighted with different colors. All the above items are
 891 closely related to the energy production in *S. methaneseepsis* ZRK33. Abbreviations:
 892 TCA, tricarboxylic acid cycle; Urea, urea cycle; ATP, 5'-Adenylate triphosphate;
 893 ADP, adenosine diphosphate; AMP, adenosine monophosphate; CA, carbonic
 894 anhydrase; NifH, nitrogenase iron protein; Q, quinone; QH₂, ubiquinone; CysN,
 895 sulfate adenylyltransferase; Sat, sulfate adenylyltransferase; CysC, adenylyl-sulfate
 896 kinase; CysQ, 3', 5'-bisphosphate nucleotidase; CysH, phosphoadenosine
 897 phosphosulfate reductase; Sir, sulfite reductase; CysK, cysteine synthase; TST,
 898 thiosulfate/3-mercaptopyruvate sulfurtransferase; DoxA, thiosulfate dehydrogenase
 899 (quinone) small subunit; DoxD, thiosulfate dehydrogenase (quinone) large subunit;
 900 Sox, L-cysteine S-thiosulfotransferase.



901

902 **Fig. 8.** Broad distribution of genes encoding key enzymes driving assimilatory and

903 dissimilatory sulfate reduction pathways in the metagenome-assembled genomes

904 (MAGs) of Chloroflexi bacteria derived from deep-sea cold seep and hydrothermal

905 vents sediments. (A) Typical pathway of assimilatory sulfate reduction existing in

906 bacteria. (B) Typical pathway of dissimilatory sulfate reduction existing in bacteria.

907 (C) Distribution of genes encoding key enzymes involved in assimilatory and

908 dissimilatory sulfur metabolisms in deep-sea Chloroflexi MAGs and strain ZRK33.

909 The presence of enzymes involved in the sulfur metabolic pathway is indicated by

910 using red colored rectangles. Sat, sulfate adenylyltransferase; CysN, sulfate

- 911 adenylyltransferase; CysC, adenylyl-sulfate kinase; CysQ, 3', 5'-bisphosphate
912 nucleotidase; CysH, phosphoadenosine phosphosulfate reductase; Sir, sulfite
913 reductase; AsrA, AsrB and AsrC, anaerobic sulfite reductases; CysI, sulfite reductase
914 (NADPH) hemoprotein beta-component; TST, thiosulfate/3-mercaptopyruvate
915 sulfurtransferase; AprA and AprB, adenylylsulfate reductase; DsrA and DsrB,
916 dissimilatory sulfite reductase.